Journal of Medicinal Chemistry

Brief Article

pubs.acs.org/jmc

Synthesis and Structure−Activity Relationships of Phosphonic Arginine Mimetics as Inhibitors of the M1 and M17 Aminopeptidases from *Plasmodium falciparum*

Komagal Kannan Sivaraman,[†] Alessandro Paiardini,[‡] Marcin Sieńczyk,[§] Chiara Ruggeri,[‡] Christine A. Oellig,[†] John P. Dalton,[∥,⊥] Peter J. Scammells,[#] Marcin Drag,*[,▽,○] and Sheena McGowan*[,†]

[†]Department of Biochemistry and Molecular Biology, Monash University, Clayton Campus, Melbourne, VIC 3800, Australia

[‡]Dipartmento di Scienze Biochimiche "A. Rossi Fanelli", Sapienza Universita di Roma, 00185 Roma, Italy

[§]Division of Medicinal Chemistry and Microbiology, Faculty of Chemistry, Wroclaw University of Technology, Wroclaw, Poland

[∥]Institute for the Biotechnology of Infectious Diseases (IBID), University of Technology Sydney, Ultimo, Sydney NSW 2007, Australia

[⊥]Institute of Parasitology, McGill University, Sainte-Anne De Bellevue, QC H9X 3V9, Canada

[#]Monash Institute of Pharmaceutical Sciences, Monash University, Parkville Campus, Australia

[▽]Program in Apoptosis and Cell Death Research, Sanford Burnham Medical Research Institute, La Jolla, California 92037, United States

[○]Division of Bioorganic Chemistry, Faculty of Chemistry, Wroclaw University of Technology, Wroclaw, Poland

Supporting Information

ABSTRACT: The malaria parasite *Plasmodium falciparum* employs two metallo-aminopeptidases, *Pf*A-M1 and *Pf*A-M17, which are essential for parasite survival. Compounds that inhibit the activity of either enzyme represent leads for the development of new antimalarial drugs. Here we report the synthesis and structure−activity relationships of a small library of phosphonic acid arginine mimetics that probe the S1 pocket of both enzymes and map the necessary interactions that would be important for a dual inhibitor.

INTRODUCTION

Malaria is responsible for 2% of global mortalities. The discovery of new antiplasmodial compounds is necessary to overcome the spread of malaria parasites that have become resistant to currently available drugs. The *Pf*A-M1 and *Pf*A-M17 neutral aminopeptidases of the malaria parasite *Plasmodium falciparum* serve as key regulators of the intracellular amino acid pool in the blood stage of the infection within malaria cells, most likely by releasing amino acids from host-derived hemoglobin.[1−4] *Pf*A-M17 was recently shown to be also essential to the early life cycle of the parasite, prior to the onset of hemoglobin digestion, suggesting that *Pf*A-M17 may have another role outside of hemoglobin digestion.[1]

Both enzymes are validated and attractive targets for lead compound discovery and optimization.[2,4−6] Attempts to genetically knock out or knock down either the *Pf*A-M1 or *Pf*A-M17 genes have been unsuccessful,[2,7] however, agents that inhibit enzymatic activity in parasites have been shown to control both laboratory and murine models of malaria.[6] Similarly, the enzymes are conserved among all *Plasmodium* species, indicating that future therapeutics could deliver cross-species inhibition.[5]

The two enzymes are both metalloproteases but have distinct differences in the arrangement of divalent metal cations in their active site. *Pf*A-M1 tightly binds a single Zn^{2+} metal ion, whereas *Pf*A-M17 contains one tightly bound and one loosely bound Zn^{2+} metal ion.[2,8] The active site of *Pf*A-M17 also has a carbonate ion present.[5] Because chelation of the metal groups in either enzyme renders them inactive,[2,8] much attention has been placed on identifying chemical scaffolds that can effectively interact with the metal ions.

A desirable quality of a potential lead antimalarial is the ability to specifically inhibit both enzymes, as this would reduce the prospect of drug-resistant parasites emerging. Phosphonopeptides,[2,5] peptide-based bestatin analogues,[9,10] and recently an orally bioavailable hydroxamate-containing ester, CHR-2863, were also shown to be efficacious against murine malaria.[11] Hydroxamate derivatives have been described as inhibitors of *Pf*A-M1.[12,13]

Optimization of lead compounds requires a detailed biological and chemical understanding of the active site architecture of each enzyme. Our group has described the structure−activity relationship (SAR) data for some of these inhibitors,[1,2,5,10] and others have used our structures to model their compounds.[11,12] This body of work has identified key architectural and chemical requirements of the active sites of both enzymes and has revealed that the substrate binding of the two enzymes differ dramatically. Thus, *Pf*A-M1 has a broad substrate tolerance, capable of efficiently hydrolyzing neutral

Received: April 23, 2013
Published: May 28, 2013

   dx.doi.org/10.1021/jm4005972 | *J. Med. Chem.* 2013, 56, 5213−5217

and basic amino acids,[2,14,15] while *Pf*A-M17 has a narrow substrate specificity and preferentially cleaves bulky, hydrophobic amino acids.[2,15,16]

In this study, we report the synthesis and SAR of a small library of metal-chelating phosphonic acid arginine mimetics that have been varied to probe the S1 pocket of both enzymes. We have mapped the necessary interactions of these compounds within the active sites of each enzyme and correlated these with their binding kinetics to elucidate some important chemistry required for a dual inhibitor.

RESULTS AND DISCUSSION

Synthesis of Inhibitors 1−8. We have previously used phosphonic analogues to probe the structure and mechanism of inhibition for both *Pf*A-M1 and -M17.[15] We knew the phosphonic acid would chelate the zinc ion(s), allowing us to map the SAR of the arginine derivatives in the S1 pockets of both enzymes.

The target phosphonic inhibitors (**1**−**8**) were synthesized from parent Cbz-protected 1-aminoalkylphosphonate diphenyl esters which were obtained via an amidoalkylation reactions either in acetic acid[17] or in dichloromethane with copper triflate as the catalyst[18] (Scheme 1). Briefly, the synthesis of **1** started with preparation of *N*-phthaloyl protected 5-aminopentanol from phthalic anhydride and 5-aminopentanol,[19] which was further oxidized to aldehyde via the Swern method. Resulting 5-*N*-Phth-aminopentanal was used in amidoalkylation reaction in acetic acid, leading to generation of side-chain Phth-protected phosphonic analogue of lysine (Cbz-Lys(Phth)^{P}(OPh)$_2$). The phthaolyl group was removed with hydrazine and the liberated amino group was guanylated using *S*-ethyl-*N*,*N*′-di(Boc)-isothiourea as the guanylating agent. Removal of Boc-protecting groups led to generation of phosphonic homoarginine (Cbz-hArg^{P}(OPh)$_2$), which was next hydrolyzed by concentrated hydrochloric acid. Inhibitor **1** was crystallized from ethanol after addition of propylene oxide. Inhibitors **2** and **3** were obtained in a similar way with the exception that 4-aminobutyrylaldehyde diethyl acetal was used as the starting material for Cbz-Orn^{P}(OPh)$_2$ and Cbz-Arg^{P}(OPh)$_2$ syntheses. Synthesis of Cbz-protected derivatives used for the preparation of **5**, **7**, and **8** was performed as described previously,[20] which was followed by complete Cbz/ester groups deprotection as described above. The synthesis of **4** started with the preparation of methyl 2-(4-nitrophenyl)acetate followed by subsequent steps such as nitro group reduction, Boc-protection, ester group reduction to alcohol, and its oxidation to an aldehyde function. Resulting 4-(*N*-Boc-amino)phenylacetaldehyde was used for the copper triflate-catalyzed amidoalkylation reaction under mild conditions. After Boc-deprotection, the obtained Cbz-(4-NH$_2$)Phe^{P}(OPh)$_2$ was guanylated and all protective groups were hydrolyzed in refluxing hydrochloric acid, leading to final inhibitor **4** (H-(4-Gu)Phe^{P}(OH)$_2$). For the synthesis of **6**, the starting 4-(1*H*-pyrazol-1-yl)benzaldehyde, prepared from 4-fluorobenzaldehyde and pyrazole,[21] was used in amidoalkylation reaction in acetic acid. Final hydrolysis of Cbz-(4-Pyr)Phg^{P}(OPh)$_2$ in refluxing HCl led to generation of **6**.

Scheme 1. General Approach for the Synthesis of Phosphonic Arginine Mimetics[a]

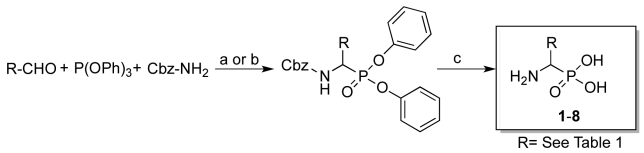

[a]Reagents and conditions: (a) acetic acid, 80−90 °C, 2 h; (b) Cu(OTf)$_2$, CH_2Cl_2, rt, 14 h; (c) conc HCl, reflux, 12 h.

***Pf*A-M1 Inhibition and SAR.** Compounds **1**−**8** were tested for their ability to inhibit *Pf*A-M1 by calculating a K_i for each compound (Table 1). **3**, **4**, and **8** were found to be not inhibitory for the enzyme. The most potent inhibitor was **1** with a K_i in the low micromolar range, while the least inhibitory compound was **7** with a K_i at 345 μM (Table 1).

Table 1. Inhibition of *Pf*A-M1 and *Pf*A-M17 by 1−8

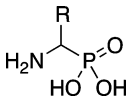

#	-R	K_i [μM] *r*PfA-M1	K_i [μM] *r*PfA-M17
1	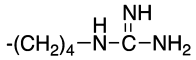	11	268
2	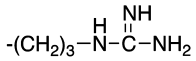	193	> 1000
3	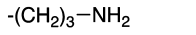	> 1000	> 1000
4	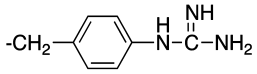	> 1000	63
5	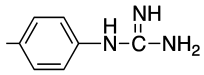	127	1.8
6	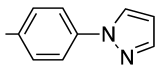	104	0.011
7	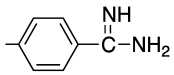	345	> 1000
8	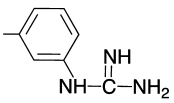	> 1000	0.16

We determined the high resolution X-ray crystal structures of each of the inhibitory compounds bound to *Pf*A-M1 (see Supporting Information (SI) Table 1 for crystallization and refinement details, Figure 1). The *Pf*A-M1 enzyme has a canonical alanyl-aminopeptidase fold with four domains. The catalytic domain contains an essential zinc ion that is well coordinated by a catalytic triad of residues His496, His500, and Glu519. Each of the compounds showed the same interactions with the zinc ion with the inhibitors primarily interacting via metallo-bonds to the O1 and O3 oxygen of the phosphate group. A further H-bond common to all inhibitors was noted between the O1 atom in the phosphate group and the −OH of Tyr580. With the exception of **7**, water molecules contributed two further interactions with the phosphate group through H-bonds with the O2 atom. The inhibitor's amine group (N4) formed 3 H-bonds with the OE oxygens of Glu319, 463, and 519. **7** was again missing a H-bond, forming interactions with only Glu319 and 519.

The most potent inhibitor was homoarginine derivative **1** with the 1-amino-5-guanidinopentyl group in a side-chain. The

dx.doi.org/10.1021/jm4005972 | J. Med. Chem. 2013, 56, 5213−5217

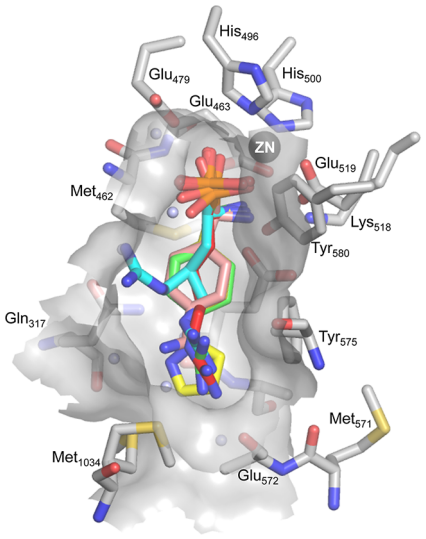

Figure 1. Diagram of inhibitors binding to active site of *Pf*A-M1. Carbon atoms of *Pf*A-M1 residues are colored in gray. Zinc is shown as black sphere, water as blue sphere. **1**–**8** are colored by carbon atom, **1** (red, 4K5L), **2** (cyan, 4K5M), **5** (green, 4K5N), **6** (yellow, 4K5O), and **7** (pink, 4K5P).

5-carbon chain showed a 10-fold increase in its K_i compared to arginine derivative **2** (Table 1). A comparison of the bound structures of these two compounds demonstrates that **1** is long enough to place the guanidino group in reach of Glu572, a key residue in the formation of the S1 pocket of *Pf*A-M1.[10] Indeed, in the crystal structure of *Pf*A-M1-**1** (PDB 4K5L), a H-bond is present between N2 and the backbone oxygen of Glu572.[2] In this structure, the side-chain of Glu572 remains unresolved, a feature common to the crystal structures of *Pf*A-M1 (SI Figure 1A).[10] The S1 pocket of *Pf*A-M1 has been shown to possess a plasticity that allows for substantial inhibitor-induced rearrangement of Glu572.[10] Neither **1** nor **2** PDB in this study altered the c–α position of Glu572. The crystal structure of *Pf*A-M1-**2** (PDB 4K5M) shows that **2** can occupy two alternative positions in the active site, identifying the reason for the reduced potency observed with this inhibitor (SI Figure 1B). The electron density clearly demonstrated that the compound branched at the C3 position, with one position occupying the same position as **1** and the second reaching away to form a H-bond with the backbone O of Val459 (SI Figure 1B). The shorter carbon chain fails to reach the Glu572 residue. Both of these structures show an alternative position for the Val459 residue in comparison to the unbound *Pf*A-M1 (PDB 3EBG) and other inhibitor bound structures.[1,2,10] The side-chain position in these structures points away from the active site and results in minor changes in the c–α backbone of the pocket (SI Figure 1C). This moves the backbone oxygen into a position where it can form the H-bond with **2** (SI Figure 1B,C). The amino group of the 4-carbon chain noninhibitory compound **3** simply lacks the ability to interact with the S1 pocket.

Compounds **5**–**8** all contain a phenyl group. **4** and **8** were noninhibitory, and both contained a rigid phenyl group with a 2-(4-guanidinophenyl) (**4**) or a 3-guanidinophenyl (**8**). This confirms the preference of *Pf*A-M1 for a straight chain P1 residue or functional group. **5** and **6** contained a 4-guanidiophenyl and a (1*H*-pyrazol-1yl) phenyl, respectively, but had equivalent K_i values. The guanidino nitrogens of **5** form H-bonds with Glu572 and Glu319, as well as two water molecules (PDB 4K5N). **6** only forms a H-bond with the O-atom of Glu319 and one water molecule. Moreover, the pyrazole moiety of **6** makes hydrophobic contacts with the side-chain of Met1034, completely filling the cleft (PDB 4K5O). Although **7** forms a similar H-bond with Glu319, this is not stabilized by any further interactions with the protein or water and is the likely reason for its reduced potency (PDB 4K5P).

***Pf*A-M17 Inhibition and SAR.** Arginine is not a substrate for *Pf*A-M17,[15] and we were interested to see if the Arg mimetics were inhibitory against the aminopeptidase. **1**–**8** were tested for their ability to inhibit the *Pf*A-M17 aminopeptidase by calculating a K_i for each compound (Table 1). Compounds with smaller groups, **2**, **3**, and **7**, were not inhibitory. The most potent inhibitor was **6** with a K_i of 11 nM, while the least inhibitory compound was **1** with a K_i at 268 μM (Table 1). With the exception of **1**, the inhibitors all displayed a K_i in the lower μM to nM range. This immediately told us that although *Pf*A-M17 had a requirement for a hydrophobic arm to satisfy the hydrophobic nature of S1 pocket in *Pf*A-M17, that inhibition of the enzyme was possible with a polar compound.

To investigate how the guanidino groups were being accommodated within the active site and S1 pocket, we attempted to determine the X-ray crystal structures of each of the compounds bound to the *Pf*A-M17. Despite extensive efforts, the only compound that was successfully crystallized with *Pf*A-M17 was **6** (see SI Table 1 for crystallization and refinement details, Figure 2, PDB 4K3N). **6** showed extensive

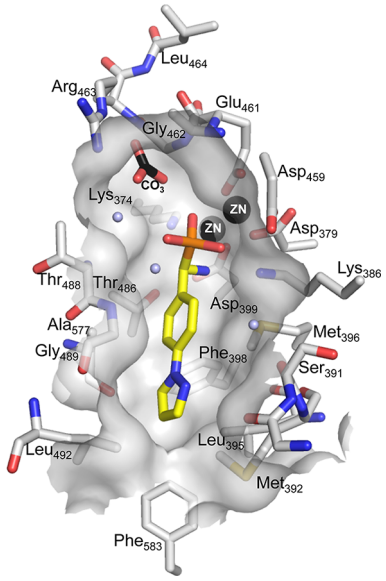

Figure 2. Diagram of **6** binding to *Pf*A-M17 (4K3N). Colors as per Figure 1.

interactions of its phosphate group with the two metal ions and carbonate ion present in each active site of *Pf*A-M17 (Figure 2). Both zinc ions and the carbonate ion formed a metal bond with O1, while O2 formed a metal bond with only one of the zinc ions but also engaged the side-chain of Lys386. The amine group of the compound formed H-bonds with Asp379 and 399. The functional group in **6** formed no further interactions with the enzyme. The 4-(1*H*-pyrazol-1-yl)phenyl group fitted neatly into the hydrophobic S1 pocket, efficiently filling the cavity (Figure 2) but forming no H-bonds, only hydrophobic packing interactions.

dx.doi.org/10.1021/jm4005972 | *J. Med. Chem.* 2013, 56, 5213–5217

To examine the interactions of the remaining compounds, we used our atomic data from the cocrystal structure of *Pf*A-M17-**6** to perform template-based molecular docking of the remaining compounds.[22] Template docking can be used when knowledge about the 3D conformation of a ligand is already available. Features expected to be relevant for the binding of the known ligand are extracted and used as energy constraints during the docking procedure. This allows the docking engine to focus the search on poses similar to the docking template, taking at the same time the ligand's flexibility into account. By utilizing active site interactions (zinc, carbonate, and *Pf*A-M17 residues) of **6** that are plausibly shared with the other compounds (phosphate and amino groups), we were able to generate models for each of them. With the exception of **1**, the compounds were docked into a single conformation within the active site. **1** was seen to have two equivalent conformations and both were subsequently analyzed.

The docking experiments revealed that positioning of the ligand with respect to the hydrophobic surface of the S1 cavity is key for potency. **7** was noninhibitory, and its carbaminidoylphenyl was shown to pack directly against the hydrophobic residues of the cavity. The positively charged guanidino group in **4** is in close proximity with the hydrophobic residues Met392, Leu492, and Phe583. Although it is likely that subtle structural rearrangements would occur to accommodate the side-chain of **4** into the hydrophobic cleft, this scenario presumably accounts for the observed reduced potency of the latter. Compared to **4**, **5** is able to shift the position of the positively charged group, moving the head moiety away from Phe583 and placing the guanidine group at favorable hydrogen-bonding distance (~2.8 Å) with the O atom of Ala577. Finally, the *meta*- substitution of **8** pushes its guanidino headgroup aside from the hydrophobic cleft formed by Met392, Leu492, and Phe583 and places it in a similar pose to that of **1** (position 2, see below), where the N3/N4 can form H-bonds with the backbone O of Gly390. This favorable interaction probably accounts for the observed increase inhibitory property, K_i = 0.16 μM, of the latter.

The straight carbon backbones proved to be relatively ineffective at inhibiting *Pf*A-M17. Only the 5-carbon chain in **1** was found to be moderately inhibitory. The two positions within the active site of *Pf*A-M17, identified by molecular docking, show that the guanidino group reaches out toward the center of the active site cavity. Position 1 (SI Figure 1) shows that the ligand can occupy a similar space to **6**, sitting effectively in the middle of the S1 cavity (SI Figure 1B). In this position, however, the guanidino group is close to the top of the S1 pocket, in particular to Ala577. Position 2 indicates that the compound could also reach away from the highly hydrophobic surface at the back of the pocket, forming a H-bond with the backbone O of Ser391 (SI Figure 2B). Analysis of docked models of the noninhibitory **2** and **3** show that the shorter carbon chains position the respective guanidino and amino groups in close proximity to the hydrophobic surface of the cavity, in particular to Phe398 and Phe583.

CONCLUSION

Aminophosphonates have been identified as potent inhibitors of the aminopeptidases for more than two decades.[23] They are simple analogues of amino acids, in which the carboxy group is exchanged for phosphonate, mimicking the transition state of the peptide bond hydrolysis. Aminophosphonates are considered as dual inhibitors, in which phosphonate fragment is responsible for binding to the zinc ion(s) in the enzyme's active site, while the side-chain binds specifically to S1 pocket of the aminopeptidase. In our work, we have demonstrated a series of aminophosphonic acid derivatives have been prepared and evaluated as inhibitors of the *Pf*A-M1 and *Pf*A-M17 aminopeptidase enzymes of *P. falciparum*. 1-Amino-5-guanidinopentylphosphonic acid (**1**) proved to be the most potent inhibitor of *Pf*A-M1, with a K_i value of 11 μM. Reduction of the length of the carbon backbone or rigidification via the incorporation of a phenyl group significantly reduced *Pf*A-M1 inhibitory activity. Similarly, retention of the guanidino groups also proved to be important for *Pf*A-M1 inhibitory activity. In contrast, 4-(pyrazol-1-yl)phenyl)(amino)methylphosphonic acid (**6**) was found to be the most potent inhibitor of *Pf*A-M17, with a K_i value in the low nanomolar range (11 nM). Encouragingly, this compound also possessed modest inhibitory activity against *Pf*A-M1 (K_i 104 μM), forming few interactions with the large S1 pocket of this enzyme. This compound supports the feasibility of developing dual *Pf*A-M1/M17 inhibitors. The scaffold of **6** has considerable scope for further optimization, both in terms of enhancing its *Pf*A-M1 inhibitory activity and its physicochemical properties for parasite killing.

EXPERIMENTAL SECTION

Chemistry. A full description of materials and details of synthetic protocol as well as spectroscopic analysis for every compound can be found in SI. A representative example of target compound **6** synthesis is described below. The purity of final compounds was examined by HPLC (Dionex, Ultimate 3000, C8 column, SunFire Prep C8 column, 10 mm × 250 mm, 5 μm, Supelco, Poland) and was greater than 95%.

The synthesis of **6** started with preparation of 4-(1*H*-pyrazol-1-yl)benzaldehyde.[21] Briefly, anhydrous K_2CO_3 (22 mmol) was suspended in DMSO (20 mL) and placed in an ultrasonic bath for 30 min. Next, 4-fluorobenzaldehyde (22 mmol) and pyrazole (20 mmol) were added and kept in an ultrasonic bath until the temperature dropped to 80 °C (1−2 h) and then was heated at 100 °C for 3 h. The reaction mixture was then extracted with diethyl ether (25 mL) and chloroform (3 × 100 mL). The ether fraction was discarded, and the combined chloroform fractions were washed with water and brine, dried over $MgSO_4$, filtered, and evaporated to dryness. The product was crystallized from hexane as a pale-yellow solid (56%). Next, the 4-(1*H*-pyrazol-1-yl)benzaldehyde (11 mmol), triphenyl phosphite (10 mmol), and benzyl carbamate (11 mmol) were dissolved in glacial acetic acid (25 mL) and heated at 80−90 °C for 2 h.[17] The solvent was evaporated, and the resulting oil was dissolved in methanol (100 mL) and left at −20 °C for crystallization. The product (Cbz-(4-Pyr)Phg^P(OPh)$_2$) was obtained as a white solid (53%). Finally, acid hydrolysis of Cbz-(4-Pyr)Phg^P(OPh)$_2$ (1.26 mmol, 1 g) led to generation of **6** as a white solid (29%), mp 278 °C.

Biochemistry. Recombinant *Pf*A-M1 and *Pf*A-M17 were produced as described previously.[2,5] Aminopeptidase activity of both enzymes and calculations of K_i are described in the SI. Co-crystallization of enzymes was achieved by the addition of 1 mM compound. Data collection and refinement statistics are available in the SI. Raw data is available from TARDIS (www.tardis.edu.au).[24] Molecular docking methods are described in the SI.

ASSOCIATED CONTENT

Supporting Information

Experimental procedures for synthesized compounds and protein crystallography including data collection and refinement statistics. Figures detailing interactions of each compound for each model generated. This material is available free of charge via the Internet at http://pubs.acs.org.

Accession Codes

PDB IDs: 4K5L, 4K5M, 4K5N, 4K5O, 4K5P, 4K3N.

AUTHOR INFORMATION

Corresponding Author

*For M.D.: phone, +48 71 3204526; fax, +48 71 3202427; E-mail, marcin.drag@pwr.wroc.pl. For S.M.: phone, +613 99029309; fax, +613 99029500; E-mail, Sheena.McGowan@monash.edu.

Author Contributions

All authors have given approval to the final version of the manuscript. K.K.S. and A.P. contributed equally.

Notes

The authors declare no competing financial interest.

ACKNOWLEDGMENTS

M.D. is grateful to the Foundation for Polish Science for financial support. S.M. is an Australian Research Council Future Fellow. We thank the NHMRC and the ARC for funding support. We thank the Australian Synchrotron (MX-1 and MX-2) and the beamline scientists for beamtime and for technical assistance. We thank the Monash Platforms (Protein Production and Crystallization) for technical assistance.

REFERENCES

(1) Harbut, M. B.; Velmourougane, G.; Dalal, S.; Reiss, G.; Whisstock, J. C.; Onder, O.; Brisson, D.; McGowan, S.; Klemba, M.; Greenbaum, D. C. Bestatin-based chemical biology strategy reveals distinct roles for malaria M1- and M17-family aminopeptidases. *Proc. Natl. Acad. Sci. U. S. A.* **2011**, *108*, E526−E534.

(2) McGowan, S.; Porter, C. J.; Lowther, J.; Stack, C. M.; Golding, S. J.; Skinner-Adams, T. S.; Trenholme, K. R.; Teuscher, F.; Donnelly, S. M.; Grembecka, J.; Mucha, A.; Kafarski, P.; Degori, R.; Buckle, A. M.; Gardiner, D. L.; Whisstock, J. C.; Dalton, J. P. Structural basis for the inhibition of the essential *Plasmodium falciparum* M1 neutral aminopeptidase. *Proc. Natl. Acad. Sci. U. S. A.* **2009**, *106*, 2537−2542.

(3) Stack, C. M.; Lowther, J.; Cunningham, E.; Donnelly, S.; Gardiner, D. L.; Trenholme, K. R.; Skinner-Adams, T. S.; Teuscher, F.; Grembecka, J.; Mucha, A.; Kafarski, P.; Lua, L.; Bell, A.; Dalton, J. P. Characterization of the *Plasmodium falciparum* M17 leucyl aminopeptidase. A protease involved in amino acid regulation with potential for antimalarial drug development. *J. Biol. Chem.* **2007**, *282*, 2069−2080.

(4) Dalal, S.; Klemba, M. Roles for two aminopeptidases in vacuolar hemoglobin catabolism in *Plasmodium falciparum*. *J. Biol. Chem.* **2007**, *282*, 35978−35987.

(5) McGowan, S.; Oellig, C. A.; Birru, W. A.; Caradoc-Davies, T. T.; Stack, C. M.; Lowther, J.; Skinner-Adams, T.; Mucha, A.; Kafarski, P.; Grembecka, J.; Trenholme, K. R.; Buckle, A. M.; Gardiner, D. L.; Dalton, J. P.; Whisstock, J. C. Structure of the *Plasmodium falciparum* M17 aminopeptidase and significance for the design of drugs targeting the neutral exopeptidases. *Proc. Natl. Acad. Sci. U. S. A.* **2010**, *107*, 2449−2454.

(6) Skinner-Adams, T. S.; Lowther, J.; Teuscher, F.; Stack, C. M.; Grembecka, J.; Mucha, A.; Kafarski, P.; Trenholme, K. R.; Dalton, J. P.; Gardiner, D. L. Identification of phosphinate dipeptide analog inhibitors directed against the *Plasmodium falciparum* M17 leucine aminopeptidase as lead antimalarial compounds. *J. Med. Chem.* **2007**, *50*, 6024−6031.

(7) Klemba, M.; Gluzman, I.; Goldberg, D. E. A *Plasmodium falciparum* dipeptidyl aminopeptidase I participates in vacuolar hemoglobin degradation. *J. Biol. Chem.* **2004**, *279*, 43000−43007.

(8) Maric, S.; Donnelly, S. M.; Robinson, M. W.; Skinner-Adams, T.; Trenholme, K. R.; Gardiner, D. L.; Dalton, J. P.; Stack, C. M.; Lowther, J. The M17 leucine aminopeptidase of the malaria parasite *Plasmodium falciparum*: importance of active site metal ions in the binding of substrates and inhibitors. *Biochemistry* **2009**, *48*, 5435−5439.

(9) Harbut, M. B.; Velmourougane, G.; Reiss, G.; Chandramohanadas, R.; Greenbaum, D. C. Development of bestatin-based activity-based probes for metallo-aminopeptidases. *Bioorg. Med. Chem. Lett.* **2008**, *18*, 5932−5936.

(10) Velmourougane, G.; Harbut, M. B.; Dalal, S.; McGowan, S.; Oellig, C. A.; Meinhardt, N.; Whisstock, J. C.; Klemba, M.; Greenbaum, D. C. Synthesis of new (−)-bestatin-based inhibitor libraries reveals a novel binding mode in the S1 pocket of the essential malaria M1 metalloaminopeptidase. *J. Med. Chem.* **2011**, *54*, 1655−1666.

(11) Skinner-Adams, T. S.; Peatey, C. L.; Anderson, K.; Trenholme, K. R.; Krige, D.; Brown, C. L.; Stack, C.; Nsangou, D. M.; Mathews, R. T.; Thivierge, K.; Dalton, J. P.; Gardiner, D. L. The aminopeptidase inhibitor CHR-2863 is an orally bioavailable inhibitor of murine malaria. *Antimicrob. Agents Chemother.* **2012**, *56*, 3244−3249.

(12) Deprez-Poulain, R.; Flipo, M.; Piveteau, C.; Leroux, F.; Dassonneville, S.; Florent, I.; Maes, L.; Cos, P.; Deprez, B. Structure−activity relationships and blood distribution of antiplasmodial aminopeptidase-1 inhibitors. *J. Med. Chem.* **2012**, *55*, 10909−10917.

(13) Flipo, M.; Beghyn, T.; Leroux, V.; Florent, I.; Deprez, B. P.; Deprez-Poulain, R. F. Novel selective inhibitors of the zinc plasmodial aminopeptidase PfA-M1 as potential antimalarial agents. *J. Med. Chem.* **2007**, *50*, 1322−1334.

(14) Allary, M.; Schrevel, J.; Florent, I. Properties, stage-dependent expression and localization of *Plasmodium falciparum* M1 family zinc-aminopeptidase. *Parasitology* **2002**, *125*, 1−10.

(15) Poreba, M.; McGowan, S.; Skinner-Adams, T.; Trenholme, K. R.; Gardiner, D. L.; Whisstock, J. C.; To, , J.; Salvesen, G. S.; Drag, M.; Dalton, J. P. Fingerprinting the substrate specificity of M1 and M17 neutral aminopeptidases of human malaria, *Plasmodium falciparum*. *PloS One* **2012**, *2*, e31938.

(16) Cunningham, E.; Drag, M.; Kafarski, P.; Bell, A. Chemical target validation studies of aminopeptidase in malaria parasites using alpha-aminoalkylphosphonate and phosphonopeptide inhibitors. *Antimicrob. Agents Chemother.* **2008**, *52*, 3221−3228.

(17) Oleksyszyn, J.; Subotkowska, L.; P., M. Diphenyl 1-amino-alkanephosphonates. *Synthesis* **1979**, *12*, 985−986.

(18) Joossens, J.; Van der Veken, P.; Lambeir, A.-M.; Augustyns, K.; Haemers, A. Development of irreversible diphenyl phosphonate inhibitors for urokinase plasminogen activator. *J. Med. Chem.* **2004**, *47*, 2411−2413.

(19) Jackson, D. S.; Fraser, S. A.; Ni, L.-M.; Kam, C.-M.; Winkler, U.; Johnson, D. A.; Froelich, C. J.; Hudig, D.; Powers, J. C. Synthesis and evaluation of diphenyl phosphonate esters as inhibitors of the trypsin-like granzymes A and K and mast cell tryptase. *J. Med. Chem.* **1998**, *41*, 2289−2301.

(20) Sieńczyk, M.; Oleksyszyn, J. A convenient synthesis of new α-aminoalkylphosphonates, aromatic analogues of arginine as inhibitors of trypsin-like enzymes. *Tetrahedron Lett.* **2004**, *45*, 7251−7254.

(21) Magdolen, P.; Mačiarová, M.; Toma, Š. Ultrasound effect on the synthesis of 4-alkyl-(aryl)aminobenzaldehydes. *Tetrahedron* **2001**, *57*, 4781−4785.

(22) Thomsen, R.; Christensen, M. MolDock: a new technique for high-accuracy molecular docking. *J. Med. Chem.* **2006**, *49*, 3315−3321.

(23) Giannousis, P. P.; Bartlett, P. A. Phosphorus amino acid analogues as inhibitors of leucine aminopeptidase. *J. Med. Chem.* **1987**, *30*, 1603−1609.

(24) Androulakis, S.; Schmidberger, J.; Bate, M. A.; DeGori, R.; Beitz, A.; Keong, C.; Cameron, B.; McGowan, S.; Porter, C. J.; Harrison, A.; Hunter, J.; Martin, J. L.; Kobe, B.; Dobson, R. C.; Parker, M. W.; Whisstock, J. C.; Gray, J.; Treloar, A.; Groenewegen, D.; Dickson, N.; Buckle, A. M. Federated repositories of X-ray diffraction images. *Acta Crystallogr., Sect. D: Biol. Crystallogr.* **2008**, *D64*, 810−814.